

Supplementary Information for: Structure and Dynamics of Stereo-regular Poly(methyl-methacrylate) Melts Through Atomistic Molecular Dynamics Simulations

Alireza F. Behbahani,^{a,b} S. Mehdi Vaez Allaei,^{*c,b} Ghodrattollah H. Motlagh,^a Hossein Eslami,^d and Vagelis A. Harmandaris^{*e,f}

^a School of chemical Engineering, College of Engineering, University of Tehran, Tehran 11155-4563, Iran

^b School of Physics, Institute for Research in Fundamental Sciences (IPM), Tehran 19395-5531, Iran

^c Department of Physics, University of Tehran, , Tehran 14395-547, Iran

^d Department of Chemistry, College of Sciences, Persian Gulf University, Boushehr 75168, Iran

^e Department of Mathematics and Applied Mathematics, University of Crete, Heraklion GR-71110, Greece

^f Institute of Applied and Computational Mathematics, Foundation for Research and Technology - Hellas, Heraklion GR-71110, Greece

The employed parameter set for simulation of PMMA is reported in Table S1. Only the first and second bonded neighbors are excluded for the calculation of the non-bonded interactions.

The value of $K_{dihedral}$ for ester-methyl dihedral angle (H1-CX-OS-C) in the original force field paper is -0.6270 (kJ/mol). Due to the considerable difference of the torsional energy profile between molecular mechanics and quantum chemistry calculations (for methyl formate) as provided in the original paper of the force field Kirschner *et al.* (2012), we decided to modify this torsional parameter to better described the ester-methyl rotation in PMMA. The prediction of (H1-CX-OS-C) torsional energy by OPLS force field Price *et al.* (2001) has been validated by comparison with quantum chemistry calculations (for methyl acetate). So, we performed a simulation of PMMA with OPLS force field and

Table S1: Force field parameters for PMMA.

non-bonded parameters			
LJ(6-12), coulomb			
atom	σ (nm)	ϵ (kJ/mol)	q (e)
CX ^a (-CH ₃ , -CH ₂ -)	0.339967	0.457730	0.0051
CX(α carbon)	0.339967	0.457730	0.0189
CX(ester-methyl)	0.339967	0.457730	0.2801
HC ^b	0.2649533	0.065689	0
C ^c	0.339967	0.359824	0.7464
O ^d	0.2959922	0.878640	-0.5939
OS ^e	0.3000012	0.711280	-0.4617
H1 ^f	0.2471353	0.065689	0
bond stretching			
$U_{bond} = \frac{1}{2}K_{bond}(r - r_0)^2$			
bond	r_0 (nm)	K_{bond} (kJ/(mol nm ²))	
CX-CX	0.152	259408.0	
CX-C	0.15	276144.0	
C-O	0.1204	835963.2	
C-OS	0.1343	344175.9	
OS-CX	0.141	267776.0	
angle bending			
$U_{angle} = \frac{1}{2}K_{angle}(\theta - \theta_0)^2$			
angle	θ_0 (deg)	K_{angle} (kJ/(mol deg ²))	
CX-CX-CX	113.5	376.6	
CX-CX-Hc	112.6	376.6	
HC-CX-HC	109.5	334.7	
CX-CX-C	111.5	334.7	
CX-C-O	125.4	493.7	
CX-C-OS	111	418.4	
O-C-OS	122.5	861.9	
C-OS-CX	114	423.4	
OS-CX-H1	110	502.1	
H1-CX-H1	109.5	376.6	
dihedral potential			
$U_{dihedral} = \sum_n K_{dihedral}^n (1 + \cos(n\phi))$			
dihedral	n	$K_{dihedral}$ (kJ/(mol))	
CX-CX-CX-CX	1	1.8828	
CX-CX-CX-HC	3	0.4184	
CX-CX-CX-C		0	
HC-CX-CX-C	3	-0.12552	
CX-CX-C-O	2	-1.7154	
	3	-1.2134	
CX-CX-C-OS	2	-1.8828	
	3	-1.3807	
O-C-OS-CX	2	-17.61464	
	3	-3.05432	
CX-C-OS-CX	1	-2.7196	
	2	-11.506	
H1-CX-OS-C	3	0.6276	

^a sp³ aliphatic carbon;^b hydrogen (except ester side group)^c sp² carbonyl carbon;^d carbonyl oxygen;^e ester oxygen;^f ester side group hydrogen

Table S2: Predicted densities of atactic PMMA with different simulation settings

effect of time step	
time step (fs)	density(kg/m ³)
2	1014
1	1011
0.1	1008
effect of constrained bonds	
type of constraining	density(kg/m ³)
flexible bonds	1013
h-bonds constrained	1014
all bonds constrained	1055

then changed the value of $K_{dihedral}$ of the present force field to be consistent with the results of OPLS simulation. The final value for $K_{dihedral}$ of (H1-CX-OS-C) dihedral was 0.6270 (kJ/mol) as reported in Table S1.

To check the effect of the simulation settings on the results, we conducted several runs with different time steps with constrained and flexible bonds. The predicted densities of atactic PMMA are reported in Table S2.

Significant effect of total bond constraining on the density of PMMA is clear from Table S2. The origin of this alteration is the difference of the backbone bond length between fully flexible and fully constrained models. The average backbone bond length is 1.59 and 1.52 Å for flexible and fully constrained models, respectively. By examining different systems we found that the nonbonded interactions between backbone atoms which are far apart by 3 bonds (1 – 4 interaction) have an important contribution to change of density by backbone bond length. The distributions of 1 – 4 distance for flexible and constrained model, are shown in Figure S1.

Conformational energy, ΔE , for each case of the single bond, diad, or inter-diad conformation, has been calculated as the weighted (with population) average energies of the *gauch* containing states relative to t , tt , or $t|t$ states, respectively. In the case of diad conformation, ΔE is calculated as,

$$\Delta E = \frac{f_i E_i}{\sum_i f_i}, \quad E_i = -RT \ln\left(\frac{f_i}{f_{tt}}\right), \quad i \in \{tg^+, g^+t, tg^-, g^-t, g^+g^-, g^-g^+, g^+g^+, g^-g^-\} \quad (1)$$

here, f_i and E_i are the fraction and energy of each conformational state, respectively.

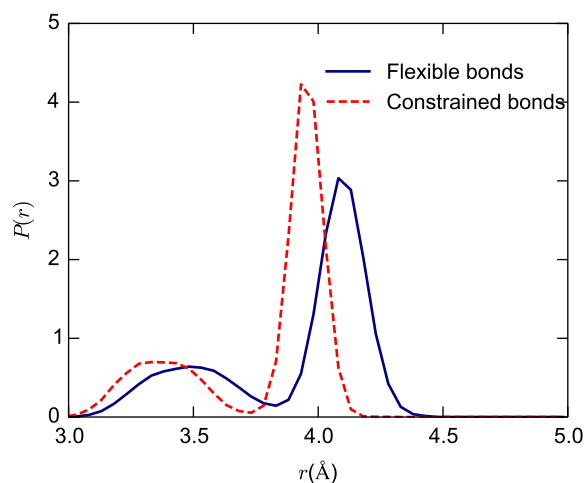


Figure S1: Distribution of 1 – 4 distance for backbone carbons for flexible and constrained models.

The internal distances of three PMMA stereo-isomers which show the distances of backbone atoms from one end of the chain ($\frac{\langle R_i^2 \rangle}{il^2}$ vs i , i is the number of backbone bonds) are shown in Figure S2.

Figure S3 shows $g_{C_b, C_b}^{intra}(r)$ for different stereo-isomers.

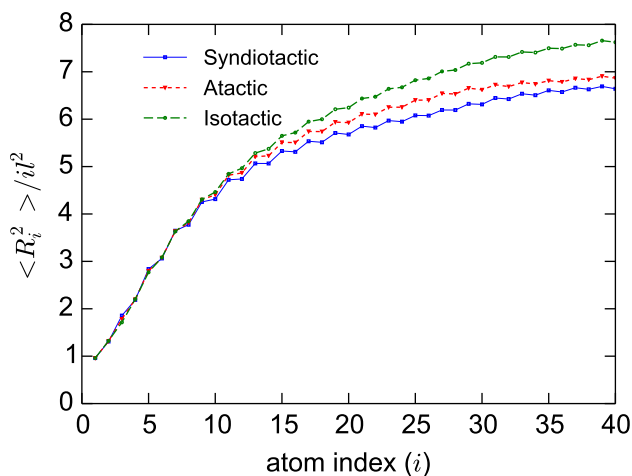


Figure S2: Internal distances of three PMMA model systems.

References

K. N. Kirschner, R. D. Lins, A. Maass and T. A. Soares, *J. Chem. Theory Comput.*, 2012, **8**, 4719–4731.

M. L. Price, D. Ostrovsky and W. L. Jorgensen, *J. Comput. Chem.*, 2001, **22**, 1340–1352.

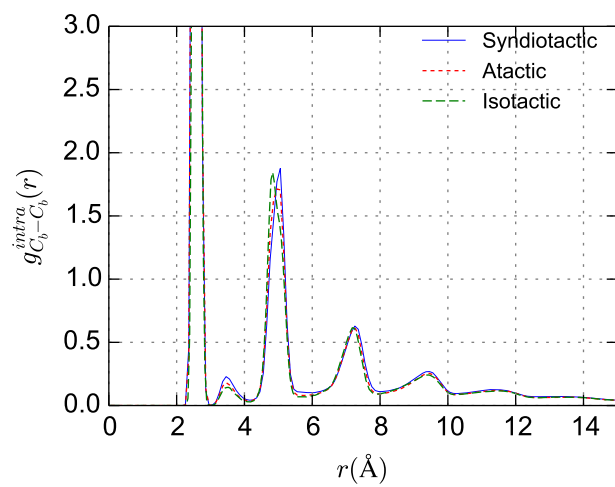


Figure S3: g_{C_b, C_b}^{intra} at 520 K.